Vacuum Squeezing of Solids: Macroscopic Quantum States Driven by Light Pulses

G. A. Garrett, A. G. Rojo, A. K. Sood,* J. F. Whitaker, R. Merlin†

Femtosecond laser pulses and coherent two-phonon Raman scattering were used to excite $KTaO_3$ into a squeezed state, nearly periodic in time, in which the variance of the atomic displacements dips below the standard quantum limit for half of a cycle. This nonclassical state involves a continuum of transverse acoustic modes that leads to oscillations in the refractive index associated with the frequency of a van Hove singularity in the phonon density of states.

Squeezing refers to a class of quantum mechanical states of the electromagnetic field and, more generally, of harmonic oscillators for which the fluctuations in two conjugate variables oscillate out of phase and become alternatively squeezed below the values for the vacuum state for some fraction of a cycle (*1*). Thus, a squeezed electromagnetic field provides a way for experimental measurements to overcome the standard quantum limit for noise imposed by vacuum fluctuations. As such, the generation of squeezed light with various nonlinear processes has attracted much attention as a means of reducing noise in optical interferometry and light-communication networks (*1*).

Following the work on photons (*1*), a variety of intriguing proposals were put forward dealing with squeezed states of other bosons—particularly those associated with atomic vibrations in molecular (*2*) and condensed-matter systems (phonons) (*3*)—as well as polaritons (*4*). In addition, squeezed phonons were considered in variational approaches to the ground state of strongly correlated electron-phonon problems (*5*). Here, we report an experimental demonstration of phonon squeezing in a macroscopic system (*6*). We have generated a squeezed mechanical state by exciting a crystal, $KTaO_3$, with an ultrafast pulse of light. The measurements were performed with the standard pump-probe setup (Fig. 1). Second-order coupling of the photons with the lattice vibrations [specifically, transverse acoustic (TA) modes] amounts to an impulsive change in the phonon frequency that gives rise to squeezing; this mechanism is closely related to that used to generate two-photon coherent states in quantum optics (*7*). We monitored the squeezed state by measuring the transmission of a second (probe) pulse that is sensitive to changes in the refractive index arising from the modulations in the mean square displacement of the atomic positions. Our state comprises a continuum of modes, but the probe transmission is dominated by a single frequency associated with a van Hove singularity in the phonon density of states.

The Hamiltonian relevant to our problem is $H = \Sigma_q(H_q + U_q)$, where $H_q = (P_q^2 + \Omega_q^2 Q_q^2)/2$ is the harmonic contribution to the lattice energy and (*8, 9*)

$$U_q = -\frac{1}{4}\mathcal{P}(\mathbf{q})F^2Q_q^2 \tag{1}$$

Here, Q_q is the amplitude of the phonon of frequency Ω_q and wave vector $\mathbf{q}$, P_q is the associated canonical momentum, F is the magnitude of the electric field, $\mathcal{P} = \Sigma_{ij}\mathcal{P}_{ij}e_ie_j$, $\mathcal{P}_{ij}(\mathbf{q})$ is the second-order polarizability tensor associated with Raman scattering (RS), and $\mathbf{e} = \mathbf{F}/F$ is a unit vector (for clarity, we omit the phonon branch index). Equation 1 describes an effective interaction between two phonons of opposite momenta and two photons and reflects the quadratic term in an expansion of the electronic susceptibility in powers of atomic displacements (*10*).

The generation of the squeezed state is best understood at temperature $T = 0$. Let E denote the pump field, and consider the assumption, valid in our experiments, that the period of the relevant phonons is large compared with both the time it takes for the pulse to cross the sample and the optical pulse width τ_0, that is, we ignore the dependence of the field on position and approximate $F^2 = E^2(t) = (4\pi I_0/n_Rc)\delta(t)$ in Eq. 1 (I_0 is the integrated intensity of the pulse, n_R is the refractive index, c is the speed of the light, and δ is the Dirac delta function). Then, if ψ_q^- is the wave function (the ground state) of a given mode at $t = 0^-$ immediately before the pulse strikes, integration of the Schrödinger equation gives the wave function at $t = 0^+$

$$\psi_q^+ = \exp\left(\frac{i\xi_q\Omega_qQ_q^2}{\hbar}\right)\psi_q^- \tag{2}$$

where $\xi_q = (\pi I_0\mathcal{P}/2cn_R\Omega_q)$ and $\hbar$ is Planck's constant divided by 2π. It follows that $\langle Q_q(t)\rangle = 0$ (the brackets denote expectation value). We use the equation of motion for Q_q^2 and the initial conditions from Eq. 2 to obtain the variance

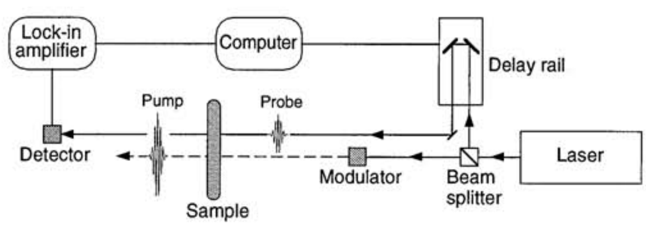

Fig. 1. Schematic snapshot diagram of the experiment (not to scale). The stronger pump pulse drives the sample into an excited time-varying state, which perturbs the weaker probe pulse that follows behind. Here, the signal of interest is the transmitted intensity of the probe beam as a function of the time delay τ, as measured by the relative distance between the two pulses.

G. A. Garrett, A. K. Sood, R. Merlin, Center for Ultrafast Optical Science, University of Michigan, Ann Arbor, MI 48109–2099, and Department of Physics, University of Michigan, Ann Arbor, MI 48109–1120, USA.
A. G. Rojo, Department of Physics, University of Michigan, Ann Arbor, MI 48109–1120, USA.
J. F. Whitaker, Center for Ultrafast Optical Science, University of Michigan, Ann Arbor, MI 48109–2099, USA.

*On leave from Department of Physics, Indian Institute of Science, Bangalore 560 012, India.
†To whom correspondence should be addressed.

$$\langle Q_q^2(t)\rangle = \langle Q_q^2(0)\rangle$$
$$[\mathcal{A}_q + (\mathcal{A}_q^2 - 1)^{1/2}\sin(2\Omega_q t + \varphi_q)] \quad (3)$$

Here, $\mathcal{A}_q = (1 + 2\xi_q^2)$ and $\tan(\varphi_q) = -\xi_q$. The time evolution of ψ_q can be represented by a variance trajectory (Fig. 2A), which shows squeezing similar to that obtained for the electromagnetic field in two-photon coherent states (*7*). As in the latter case, the motion described by ψ has no classical analog (*11, 12*). Parenthetically, we note that the same method can be used to reduce thermal noise, other than quantum fluctuations (Fig. 2B) (*13*). Classically, the equation of motion is $\ddot{Q}_q + \Omega_q^2 Q_q = 2\xi_q\Omega_q Q_q\delta(t)$. Thus, $Q_q(0^+) = Q_q(0^-)$, whereas $\dot{Q}_q(0^+) = \dot{Q}_q(0^-) + 2\xi_q\Omega_q Q_q(0)$. It can then be shown that the isotropic equilibrium distribution becomes an elliptical one that rotates at twice the harmonic frequency (*13*).

The previous discussion centered on the behavior of an excitation of a well-defined wave vector. However, our experiments concern themselves not with single phonon but with real-space squeezing involving an average over all of the modes. Here, we use the fact that the wave functions of the solid as a whole are $\Psi^- = \Pi_q\psi_q^-$ $(t < 0)$ and $\Psi^+ = \Pi_q\psi_q^+$ $(t > 0)$ to calculate the variance

$$\langle \mathcal{U}^2(t)\rangle = \sum_l \frac{M(l)}{M_T}\langle \mathbf{u}^2(l)\rangle = \sum_q \frac{\langle Q_q^2(t)\rangle}{NM_T} \quad (4)$$

which provides a measure of the squeezing (*14*); $\mathbf{u}(l)$ and $M(l)$ are, respectively, the deviation from equilibrium and the mass of the lth atom in the unit cell, N is the number of unit cells, and $M_T = \Sigma_l M(l)$. Because $\langle Q_q^2\rangle$ depends only on the mode frequency, **u**-space squeezing pertains to the phonon density of states, that is, the characteristic frequencies for $\langle\mathcal{U}^2\rangle$ are those of van Hove singularities where the phonon density is large. Thus, the zero-temperature description is an accurate representation of experiments performed at temperatures for which k_BT (the thermal energy; k_B is Boltzmann's constant) is very small compared with the van Hove phonon energies.

The data were obtained from a ~3 mm × 10 mm × 0.5 mm single crystal of $KTaO_3$ oriented with the [001] axis perpendicular to the large face at 10 K (*15*). As a light source, we used a mode-locked Ti-sapphire laser providing pulses of full width ≈70 fs centered at 810.0 nm at a repetition rate of 85 MHz and an average power of 60 mW focused to a 70-μm-diameter spot. Spontaneous RS measurements were recorded in the backscattering configuration with 30 mW of a continuous-wave Ti-sapphire laser also tuned to 810.0 nm, or an Ar laser operating at 514.5 nm (*16*).

The scattering of the probe pulse by the squeezed state relates to the nonlinear polarization $P_i^{NL} = \Sigma_j\chi_{ij}^R E_j'(t)$. Here, $\mathbf{E}'$ is the probe field, $\chi_{ij}^R = (2V)^{-1}\Sigma_q\mathcal{P}_{ij}\langle Q_q^2\rangle$ is the second-order Raman susceptibility, and V is the scattering volume. Consider a Gaussian-shaped probe pulse of width τ_0 centered at frequency ω_0, that is, $E_j'(u) \propto \exp[-(u^2/2\tau_0^2)]\cos(\omega_0 u)$, with $u = t - \tau$ (τ is the time delay between the pump and probe pulses). Using well-established results for coherent phonons (*17*) and in the limit $\xi_q \rightarrow 0$, which is relevant to the experiments, we obtain the τ dependence of the normalized change in the probe transmission at frequency ω

$$\frac{\Delta\mathfrak{T}}{\mathfrak{T}} \approx -\frac{4\pi\tau_0^2\omega(\omega-\omega_0)}{n_R cV}$$
$$\times \sum_q \mathcal{P}'(\mathbf{q})\Omega_q\xi_q\langle Q_q^2(0)\rangle\cos(2\Omega_q\tau)\exp(-2\Omega_q^2\tau_0^2) \quad (5)$$

where $\mathcal{P}' = \Sigma_{ij}\mathcal{P}_{ij}e_i' e_j'$ and $\mathbf{e}' = \mathbf{E}'/E'$. Using Eqs. 3 to 5 and neglecting the weak dependence of $\mathcal{P}_{ij}$ on **q**, we obtain $\partial\langle\mathcal{U}^2\rangle/\partial t \propto \Delta\mathcal{T}/\mathcal{T}$. Accordingly, the integral of $\Delta\mathcal{T}/\mathcal{T}$ probes the variance $\langle\mathcal{U}^2\rangle$, which measures the strength of the squeezing. The proportionality constant as well as $\langle\mathcal{U}^2(0)\rangle$ can be unequivocally determined from our measurements.

Time-domain results are shown in Fig. 3A. The Fourier transform $\mathcal{F}_{FT}(\Omega) = \int(\Delta\mathcal{T}/\mathcal{T})\cos(\Omega\tau)d\tau$ (Fig. 3B) is dominated by a narrow peak, strongly dependent on temperature, that appears very close to twice the frequency of the TA mode at the X point of the Brillouin zone, as measured by neutron scattering (*18*). On the basis of this peak and the comparison between the time-domain (Fig. 3B) and the spontaneous RS measurements (Fig. 3C), we ascribe the structure to the 2TA overtone. The sharpness and strength of the 2TA peak reflects to some extent the flatness of the phonon dispersion near the zone boundary (*18, 19*). For a given irreducible component, it can be shown from previously derived expressions (8, 9) that $\mathcal{F}_{FT}(\Omega) \propto \mathcal{I}(\Omega)\exp(-\Omega^2\tau_0^2/2)/C(2\Omega)$, where $\mathcal{I}(\Omega)$ is the second-order RS cross section and $C(\Omega) = (\hbar/2\Omega)[1 -$

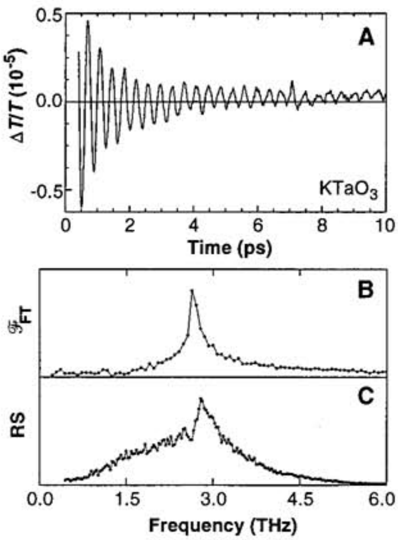

Fig. 3. (**A**) Normalized transmitted intensity of the probe pulse as a function of the delay for the A_{1g}-symmetry configuration. (**B**) Fourier transform of the time-domain data. (**C**) Weighted second-order Raman cross section $\mathcal{I}(\Omega)\exp(-\Omega^2\tau_0^2/2)/C(2\Omega)$ obtained at 810.0 nm.

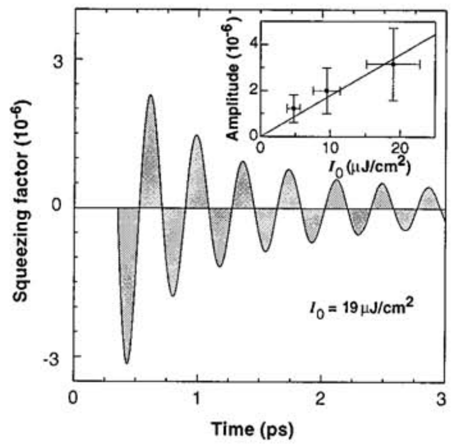

Fig. 4. Experimental time dependence of the squeezing factor $\mathcal{S} = 1 - [\langle\mathcal{U}^2(t)\rangle/\langle\mathcal{U}^2(0)\rangle]^{1/2}$ at integrated pulse intensity $I_0 = 19$ μJ/cm². (**Inset**) Amplitude of $\mathcal{S}$ as a function of I_0.

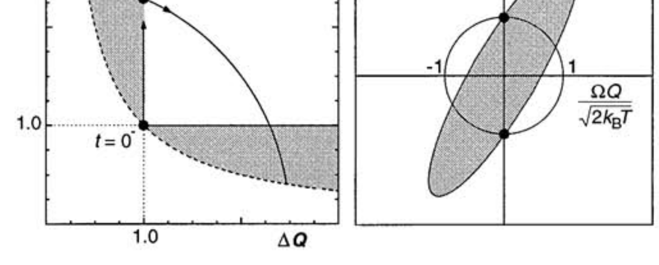

Fig. 2. (**A**) $\Delta P = \langle P^2(t)\rangle^{1/2}$ versus $\Delta Q = \langle Q^2(t)\rangle^{1/2}$ in units of $(\hbar\Omega/2)^{1/2}$ and $(\hbar/2\Omega)^{1/2}$, respectively. Dots denote values immediately before ($t = 0^-$) and after ($t = 0^+$) the pulse is applied. The circular arc is the trajectory for $t > 0$. Shaded regions represent quadrature-squeezed states. Minimum-uncertainty states lie on the hyperbola (dashed curve). (**B**) Classical phase-space diagrams showing the circular ($t < 0$) and elliptical ($t > 0$) noise distributions.

$\exp(-\hbar\Omega/k_B T)]^{-1}$. The comparison between Figs. 3B and 3C indicates that this theoretical prediction is in reasonable agreement with the experimental data. However, there are significant differences concerning the line shape that are not understood.

To further support our interpretation, as well as to provide a quantitative estimate of the variance $\langle \mathcal{U}^2 \rangle$, we obtained the absolute RS cross section by comparing $KTaO_3$ with the standard CaF_2 using the 514.5-nm laser line. From these measurements, if we ignore the dependence of the polarizability on the wave vector, we find that for the A_{1g} component, $\mathcal{P}_{11} = \mathcal{P}_{22} = \mathcal{P}_{33} = a = (6 \pm 2) \times 10^{15}$ cm/g, which compares favorably with the value $a = (4 \pm 1) \times 10^{15}$ cm/g that we obtain from the pump-probe experiments using Eqs. 3 and 5. From these values, we determine the proportionality constant relating $\partial\langle \mathcal{U}^2 \rangle/\partial t$ to $\Delta\mathcal{T}/\mathcal{T}$, and from the spontaneous RS measurements (*20*), we obtain $\langle \mathcal{U}^2(0) \rangle$, which corresponds to the standard quantum limit $\Delta P_q = \Omega \Delta Q_q = (\hbar\Omega/2)^{1/2}$. Combining these results and integrating $\Delta\mathcal{T}/\mathcal{T}$, we get $\langle \mathcal{U}^2(t) \rangle / \langle \mathcal{U}^2(0) \rangle$. In Fig. 4, we plot $\mathcal{S} = 1 - [\langle \mathcal{U}^2(t) \rangle / \langle \mathcal{U}^2(0) \rangle]^{1/2}$, which is referred to as the squeezing factor (*21*); **u**-squeezing corresponds to $\mathcal{S} > 0$. We notice that, for $\xi_q \ll 1$, Eqs. 3 and 4 predict that $\mathcal{S}$ ($\ll 1$) should be proportional to the pump energy density I_0. This prediction is well obeyed for densities in the range $I_0 \approx 5$ to 20 μJ/cm^2 (Fig. 4, inset).

REFERENCES AND NOTES

1. R. E. Slusher *et al.*, *Phys. Rev. Lett.* **55**, 2409 (1985); L. Wu *et al.*, *ibid.* **57**, 2520 (1986); D. F. Walls, *Nature* **324**, 210 (1986). See also the special issues on squeezed states: H. J. Kimble and D. F. Walls, Eds., *J. Opt. Soc. Am. B* **4** (no. 10) (1987); E. Giacobino and C. Fabre, Eds., *Appl. Phys. B* **55** (no. 3) (1992).
2. J. Janszky and Y. Y. Yushin, *Opt. Commun.* **59**, 151 (1986); J. Janszky and An. V. Vinogradov, *Phys. Rev. Lett.* **64**, 2771 (1990); J. Janszky, P. Adam, An. V. Vinogradov, T. Kobayashi, *Spectrochim. Acta A* **48**, 31 (1992).
3. X. Hu and F. Nori, *Phys. Rev. Lett.* **76**, 2294 (1996); X. Hu, thesis, University of Michigan (1996).
4. M. Artoni and J. L. Birman, *Phys. Rev. B* **44**, 3736 (1991); *Opt. Commun.* **104**, 319 (1994); X. Hu and F. Nori, *Phys. Rev. B* **53**, 2419 (1996).
5. See, for example, C. F. Lo, E. Manousakis, R. Sollie, Y. L. Wang, *Phys. Rev. B* **50**, 418 (1994); M. Sonnek and M. Wagner, *ibid.* **53**, 3190 (1996).
6. The generation of nonclassical states has been recently demonstrated for a trapped atom by D. M. Meekhof, C. Monroe, B. E. King, W. M. Itano, and D. J. Wineland [*Phys. Rev. Lett.* **76**, 1796 (1996)].
7. H. P. Yuen, *Phys. Rev. A* **13**, 2226 (1976); ______, and J. H. Shapiro, *Opt. Lett.* **4**, 334 (1979); D. F. Walls and G. J. Wilburn, *Quantum Optics* (Springer, Berlin, 1994), chap. 2.
8. M. Born and K. Huang, *Dynamical Theory of Crystal Lattices* (Clarendon, Oxford, 1954), pp. 306–319.
9. J. L. Birman, *Theory of Crystal Space Groups and Lattice Dynamics* (Springer, Berlin, 1984), pp. 282–295.
10. Such a phenomenological description relying on the Born-Oppenheimer approximation applies strictly only to insulators for which it can be easily formalized (*9*) to provide the basis of bond-polarizability models of intrabranch or overtone (*8, 9*) second-order RS. We recall that the usually dominant first-order RS is accounted for by an expression that is of the same form as Eq. 1 but is linear in Q_q, with $\mathbf{q} \approx 0$ (*8, 9*). Although the absence of first-order scattering is not required to achieve squeezing, we simplify the discussion by focusing on materials of symmetry such that the linear terms vanish. Also note that, in general, $\mathcal{P}_{ij}$ contains interbranch in addition to the intrabranch contributions shown in Eq. 1. The former have not been included because they are typically much weaker than the terms of interest (*9*).
11. Squeezing relies primarily on the fact that U_q is proportional to Q_q^2 and not so much on the particular form of the coupling to the field. Squeezing can also be obtained from the term giving two-phonon absorption, that is, $U_q = \mathbf{F} \cdot \mathcal{D}(\mathbf{q}) Q_q^2$, provided $\int F dt \neq 0$ ($\mathcal{D}$ is the second-order dipole moment).
12. These considerations can be easily generalized to include materials that exhibit first-order RS. However, there is an important distinction in that terms linear in Q_q generate states with displaced vacua, that is, $\langle Q_q \rangle \neq 0$, whereas quadratic contributions do not. Linear terms lead to one-mode coherent states [R. J. Glauber, *Phys. Rev.* **131**, 2766 (1963)], which are the closest to a classical description of the motion.
13. Classical squeezing of an oscillator was first demonstrated by D. Rugar and P. Grütter [*Phys. Rev. Lett.* **67**, 699 (1991)]. See also V. Natarajan, F. DiFilippo, D. E. Pritchard, *ibid.* **74**, 2855 (1995).
14. Depending on the experimental technique, we expect vacuum squeezing of a solid to manifest itself in different ways. In particular, the neutron or x-ray scattering structure factor is, to lowest order in the field intensity, $S(\mathbf{k}, t) \approx e^{-2W}[1 - k^2(\langle \mathcal{U}^2(t) \rangle/2 + \langle Q_k(0) Q_k(t) \rangle / M_T)]$, where e^{-2W} is the static Debye-Waller factor. Thus, S contains effects due to both **k**-space (single-mode) and, as in Eq. 4, real-space squeezing.
15. Experiments at room temperature reveal behavior that is qualitatively similar to that at 10 K. The 300-K results will be reported elsewhere.
16. $KTaO_3$ crystallizes in the cubic perovskite structure (point group O_h) with no first-order Raman active modes, that is, the leading term in the expansion of the susceptibility is given by Eq. 1. In O_h, the irreducible Raman representations are A_{1g}, E_g, and T_{2g}. We singled out the individual contributions by subtracting pairs of spectra obtained with the appropriate choice of polarization directions. Time-domain data were obtained with the polarization of the pump perpendicular to that of the probe beam and oriented along [100] or [010]. In RS, the incident and scattered light were polarized parallel to {110}. Our RS measurements are in good agreement with early experiments reported by W. G. Nielsen and J. G. Skinner [*J. Chem. Phys.* **47**, 1413 (1967)]. The time-domain and RS results reported here are for overtones that transform according to the fully symmetric component A_{1g}. We find that the behavior of the weaker E_g spectrum is similar to that of A_{1g} and that the T_{2g} contribution is negligible.
17. See, for example, L. Dhar, J. A. Rogers, K. A. Nelson, *Chem. Rev.* **94**, 157 (1994); R. Merlin, *Solid State Commun.* **102**, 207 (1997).
18. R. Comes and G. Shirane, *Phys. Rev. B* **5**, 1886 (1972).
19. The width of the 2TA feature in Fig. 3B is 0.11 ± 0.02 THz. This value gives an upper limit for lifetime effects due to anharmonicity (phonon-phonon interaction).
20. We use $\int \mathcal{I}(\Omega) C^{-1}(\Omega) d\Omega = (2\pi\omega_L^2 \mathcal{E}_L a/c)^2 N M_T \langle \mathcal{U}^2(0) \rangle$, where ω_L and $\mathcal{E}_L$ are the frequency and field of the continuous-wave laser (*8*).
21. For the variance (Eq. 4), the dominant contributions to the systematic error are the uncertainties in the polarizability (25%) and the integrated intensity of the pulse (20%). The statistical errors in Fig. 4 have been minimized by data averaging and filtering.

22. We are indebted to P. Grenier for providing the $KTaO_3$ sample and to D. G. Steel for a critical reading of the manuscript. A.K.S. would like to thank the Department of Physics at the University of Michigan for warm hospitality. Supported by the NSF through the Center for Ultrafast Optical Science under grant STC PHY 8920108 and by the U.S. Army Research Office under contract DAAH04-96-1-0183.

2 December 1996; accepted 30 January 1997